Citation: Holé, S., Dissado, L. A., Ajour, M. N. & Fothergill, J. (2005). Space charge behaviour in epoxy laminates under high constant electric field. Journal of Physics D: Applied Physics, 38(16), pp. 2890-2898. doi: 10.1088/0022-3727/38/16/022

This is the unspecified version of the paper.

This version of the publication may differ from the final published version.

Link to published version: https://doi.org/10.1088/0022-3727/38/16/022

Space charge behavior in Epoxy laminates under **high constant electric field**

Stéphane Holé*
Laboratoire des Instruments et Systèmes d'Ile de France
Université Pierre et Marie Curie - 10, rue Vauquelin, 75005 Paris - France

Leonard A. Dissado†
Department of Engineering,
University of Leicester - Leicester LE1 7RH - UK

Mohammed N. Ajour‡
University of Philadelphia - Jarash - P.O. Box 40 - Jordan

John C. Fothergill§
Department of Engineering,
University of Leicester - Leicester LE1 7RH - UK

6th June 2005

Abstract

The development of space charge in insulating materials is one of the main causes of their electrical aging. The pulsed electro-acoustic (PEA) method is often used to determine space charge distribution, but the signal analysis in the case of laminate structures is much more complex to analyze. In this paper the authors describe and use a simulated signal in order to study laminates made of Epoxy resin and fibre mat. The relatively large conductivity of the fibres compared to **that of the resin seems to produce** a rapid charge dissociation and recombination in the fibres. Under voltage the presence of fibres close to an electrode **seems to promote** charge injection.

---

*e-mail: `stephane.hole@espci.fr`
†e-mail: `lad4@le.ac.uk`
‡e-mail: `Ajour@Pheladelphia.edu.jo`
§e-mail: `jcf@le.ac.uk`

1 Introduction

The development of space charges in insulating materials is one of the main causes of their electrical aging [1], and thus of the life time reduction of the system in which they are included. The cost of repair of any electrical failure, for instance in systems underneath the soil or the sea, is so important that system life time must be as high as possible. In some systems, such as in the power feed line for optical telecommunication [2], high voltage circuits are etched on Epoxy resin boards which include a silica fibre mat. That silica fibre mat improves the mechanical strength of the board but can be detrimental to its electrical properties. This may lead for instance to premature electrical aging. It is therefore necessary to study the electrical behavior of such insulating structures in order to estimate their suitability in systems requiring a long life time.

Since space charges take part in the aging process, the measurement of their distributions is of great interest. Among the different measurement techniques [3], the Pulsed Electro-Acoustic [4, 5] (PEA) and the Pressure Wave Propagation [6, 7, 8] (PWP) methods make it possible to directly determine the distribution of space charge without requiring complex mathematical post-treatments. Although these methods provide a similar information [9], we have used the PEA method for this study. The PEA method consists in the perturbation of the material to be studied by an electric pulse and in the measurement by an adjacent transducer of the elastic waves generated in response by the material. During the perturbation, the charges in the material are indeed subjected to an extremely large variation of electrostatic forces. This results in a rapid deformation of the material which generates elastic waves propagating outward from its source, that is to say from the charges. Since elastic waves propagate at the velocity of sound, the transducer collecting one part of the emitted waves receives the waves generated by each charge at a time depending on the distance from the charge to the transducer. Therefore, the time dependence of the signal produced by the transducer is directly associated with the distribution of charges in the material, time and space being related by the velocity of sound.

In the case of complex material structures, the space charge distribution cannot be extracted from the signal generated by the implementation of the PEA method as directly as that for uniform materials. This is due to the spatial variation of other parameters contributing to the signal such as the permittivity [10, 11]. Epoxy resin boards including a fibre mat are one kind of these complex material structures since at one position in the insulating structure one finds either the electrical properties of the Epoxy resin or those of the fibre mat. As a consequence, the PEA signal must be analyzed carefully to extract only the useful information.

In this paper the PEA signal produced by an Epoxy resin board including a fibre mat is simulated and compared with measurements. By fitting the parameters of the simulation in order to match the experimental results it is possible to determine the electrical behavior of the sample. Such an approach has already been successfully used to study samples containing a divergent field region [12]. In the first section, the physical basis of the simulation is presented for a one-dimensional laminate structure. Though this approach corresponds to an Epoxy resin board including a silica fibre mat, it can almost be directly applied to any other kind of unidimensional laminate sample structures. In the following section, experimental data for Epoxy resin boards including a silica fibre mat are shown, analyzed, and discussed in order to extract the electrical behavior of such laminates when stressed by **10 kV/mm** at room temperature.

2 PEA signal simulation

2.1 Sample structure

The composite was a standard "FR4" printed-circuit board material, type N4000-2 made by Park-Nelco. The samples studied in this paper are 400 μm thick and include a double-layer silica fibre mat. The fibres are 15 μm in diameter and are arranged in two layers crossing perpendicularly every mm approximatively.

Figure 1-left is a micro-photograph of the laminate cut section. The contrast is adjusted so as to present silica fibres in white and Epoxy resin in grey. It is clearly shown that the two fibre layers in the mat are separated by Epoxy resin. As a consequence the sample can be described as containing five layers, the first, the third and the fifth being mainly Epoxy resin, and the second and the fourth being mainly Silica. This is illustrated in Figure 1-right.

All measurements presented in this paper were carried out with a sample without bonded electrodes. The electrodes are acoustically coupled to the sample by silicon oil. We verified that there is no detectable difference between measurements carried out with a sample with bonded copper electrodes and without bonded electrodes.

2.2 Signal model

A typical PEA setup is presented in Figure 2. A sample containing charges is subjected to a constant voltage stress V_a. A measurement is initiated by applying to the sample a pulsed voltage V in addition to V_a in order to generate an electric perturbation. The resulting variation of electric force acting on the material and particularly on its charges produces elastic waves which propagate in the sample structure at the velocity of sound. One part of the waves reaches an adjacent transducer converting those waves to an electric signal. Since elastic waves propagate at the velocity of sound, the transducer converts the waves produced first by the charges on the front electrode, then by the charges inside the sample, and finally by the charges on the back electrode.

Though the fine structure of the mat is not really planar, it can be considered planar in average over the lateral extent of the electrode feeding the sample with the pulsed voltage since it is much larger than the sample thickness. In this case, each layer of the sample has a dielectric constant which is closer to that of Epoxy resin in layers 1, 3 and 5 and closer to silica in layers 2 and 4 (see Figure 1-right). With such simplifications, we do not expect that measured and simulated signals to fit perfectly together, but we expect the general electrical behavior of the real structure to be extracted.

In planar geometry [9] the material deformation S at **time t and the position** z due to the waves generated by the voltage pulse is

$$S(z,t) = \int_0^d \int_{t'} \Delta M(z',t')\, G(z,z',t-t')\,\mathrm{d}t'\,\mathrm{d}z', \tag{1}$$

where d is the sample thickness**, and z' and t' are position and time relative to the sources of elastic waves. It can be noticed that the integral over t' is a convolution product.**

The Maxwell tensor variation $\Delta M(z',t')$ describes the source of elastic waves. It depends on the electrical properties of the sample structure, **particularly on the permittivity $\epsilon(z')$, and the electrostrictive constant $a(z')$, and the capacitance at rest per unit area C_0. It depends also on the electrical conditions, particularly the electric field $E(z')$, the permanently oriented dipole distribution $\pi(z')$, and the pulsed voltage $V(t')$. The permanently oriented dipole distribution $\pi(z')$ represents the part of dipoles that cannot re-orient in the electric field during the measurement time scale, typically less than a microsecond. The dipoles that can easily re-orient in the electric field in the measurement time scale are taken into account in the permittivity $\epsilon(z')$. The electric field $E(z')$ and the permanently oriented dipole distribution $\pi(z')$ in the sample may also vary in time but so slowly compared to $V(t')$ that they are considered as constant during a measurement. The z' and t' dependences are omitted hereafter to reduce the length of equations.** One has:

$$\Delta M = -\frac{C_0}{\epsilon}\left(\left(\epsilon - a\right)E + \pi\right)V + \frac{C_0^2}{2\epsilon^2}\left(\epsilon - a\right)V^2. \tag{2}$$

The Green's function $G(z, z', t - t')$ describes how elastic waves travel in the sample structure from its source at position z' to the observation point at position z. Since the sample is made of different layers, the acoustic impedance mismatches between each layer may produce reflections of elastic waves and thus **increase the complexity of the expression of G. That could result in a signal depending more on the mechanical behavior of the sample than on its electrical behavior. In order to test whether reflections occur in the laminate studied, a semi-conductive electrode was inserted at the back of the sample, and PEA measurements were carried out under 4-kV-applied voltage and under short-circuit before and after the voltage application. Short-circuit measurements are necessary to ensure that charges do not accumulate during the measurement under voltage and to determine the part of the signal which does not depend on the 4-kV-applied voltage. Since the two short-circuit measurements gave similar results, the voltage application did not cause charge to accumulate.** The signal resulting from the subtraction of the short-circuit measurement from the 4-kV measurement is presented in Figure 3. The part of the signal corresponding to the semi-conductive electrode is flat. Since the reflected waves are delayed compared to the direct waves, this part of signal should have shown significant variations if reflections occurred inside the sample structure. **Indeed if there were reflected (delayed) waves, the transducer would have produced a delayed signal which would have been superimposed on the signal corresponding to the semi-conductive electrode. The signal corresponding to the semi-conductive electrode being flat, any delayed signal produced by the reflected waves is not detectable.** It can be concluded that reflections between layers are negligible in this sample structure. **Measured signals are therefore only of electrical origin, the mechanical perturbation due to the sample structure being marginal.** As a consequence one can take the Green's function of a uniform media:

$$G(z, z', t - t') = \frac{1}{2\, v_s\, Y}\, \delta'(t - t' - \frac{z' - z}{v_s}). \tag{3}$$

In this expression v_s is the velocity of elastic waves, Y is the Young's modulus, $\delta'(\eta) = \partial\delta(\eta)/\partial\eta$ is the Dirac's function derivative, and $z < z'$. With this Green's function it is possible to calculate the material deformation S or the pressure $-YS$ at the front of the sample ($z = 0$) **by using convolution product properties with Dirac's function and its derivatives [13],** and then to determine the material deformation or pressure at the transducer position by multiplying this expression by the transmission coefficient τ of elastic waves from the sample to the transducer through the waveguide, and by applying the convenient time delay Δt corresponding to the time elastic waves take to travel through the waveguide. By introducing (2) and (3) in (1) and taking into account τ and Δt one obtains the following expression for the pressure P at the transducer position:

$$\begin{aligned} P(t) \quad = \quad & \frac{\tau\, C_0}{2\, v_s} \int_0^d \frac{(\epsilon - a)\, E + \pi}{\epsilon}\, \frac{\partial}{\partial t} V(t - \Delta t - z'/v_s)\, \mathrm{d}z' \\ & -\frac{\tau\, C_0^2}{4\, v_s} \int_0^d \frac{\epsilon - a}{\epsilon^2}\, \frac{\partial}{\partial t} V^2(t - \Delta t - z'/v_s)\, \mathrm{d}z'. \end{aligned} \tag{4}$$

At this stage it can be pointed out that the velocity of sound v_s may be slightly different from one layer to another even in the case of a perfect acoustic impedance matching. As a consequence, a given amount of time in the signal may not correspond exactly to a constant amount of space in the sample. We will see in section 2.4 that it does not really matter since the signal gives clues about the sample structure.

Attenuation and dispersion of elastic waves have not been taken into account so far. That can be done in the harmonic regime with

$$G(z,z',\omega,t-t') = \frac{\imath\, k}{2\, Y}\, e^{\imath\omega(t-t')-\imath k(z'-z)} \tag{5}$$

where ω is the angular frequency, k is the wave vector, and $\imath = \sqrt{-1}$. **Equation (5) is the Fourier transform of Equation (3). The wave vector k is often defined as $k = \omega/v_s(\omega) - \imath\alpha(\omega)$ in dispersive and lossy materials where dispersion is characterized by the variation with frequency of the velocity of sound $v_s(\omega)$ and attenuation by the factor $\alpha(\omega)$. Denoting** FT **as the Fourier transformation, the pressure at the transducer position is:**

$$\begin{aligned} P(t) \quad = \quad & \frac{\tau\, C_0}{4\pi} \int_\omega \imath\, k\, \mathrm{FT}(V) \left(\int_0^d \frac{(\epsilon - a)\, E + \pi}{\epsilon}\, e^{-\imath k z'}\, \mathrm{d}z' \right) e^{\imath\omega(t-\Delta t)}\, \mathrm{d}\omega \\ & -\frac{\tau\, C_0^2}{8\pi} \int_\omega \imath\, k\, \mathrm{FT}(V^2) \left(\int_0^d \frac{\epsilon - a}{\epsilon^2}\, e^{-\imath k z'}\, \mathrm{d}z' \right) e^{\imath\omega(t-\Delta t)}\, \mathrm{d}\omega \end{aligned} \tag{6}$$

2.3 Signal simulation

In order to simulate the pressure at the transducer position with Equation (4) or (6), at least four steps are necessary.

It is firstly necessary to determine the capacitance of the sample at rest per unit area C_0. Since the capacitance is defined as the charges brought to one electrode when the applied voltage swings from 0 to 1 V across the sample, one has

$$C_0 = 1 \bigg/ \int_0^d \frac{1}{\epsilon}\, \mathrm{d}z. \tag{7}$$

It is secondly necessary to determine the electric field from the electrical parameters and conditions of the sample. In a one-dimensional model one has:

$$\frac{\partial(\epsilon E + \pi)}{\partial z} = \rho \tag{8}$$

so that

$$E = \frac{1}{\epsilon} \int_0^z \rho(z')\, \mathrm{d}z' - \frac{\pi}{\epsilon} - \frac{C}{\epsilon}. \tag{9}$$

The constant C can be deduced by the integration of the electric field over the sample thickness which is equal to the opposite of the applied voltage V_a. One obtains:

$$C = C_0 \int_0^d \left(\frac{1}{\epsilon} \int_0^z \rho(z')\, \mathrm{d}z' - \frac{\pi}{\epsilon} \right) \mathrm{d}z + C_0 V_a. \tag{10}$$

It is thirdly necessary to determine attenuation and dispersion of the elastic waves. The frequency dependence of the attenuation and dispersion can be measured with the PEA method itself [14]. Indeed the subtraction of a signal obtained from a sample under voltage by the one obtained from the same sample under short circuit shows two peaks. **Obviously the absence charge accumulation is assumed during the voltage application.** The first peak corresponds to the front electrode response whereas the second peak corresponds to the back electrode response. Since the transit through the sample is the only difference between the travel of these two elastic wave responses, it is possible to evaluate how elastic waves attenuate and disperse from these two peaks. This technique is however difficult to apply in the case of complex samples since signals due to front and back electrodes can mix with other signal sources such as the spatial variation of permittivity which depends also on the applied voltage [11].

Another possibility is to model the degradation of the elastic wave as it propagates. It is less precise than measuring real coefficients but it is sufficient in many cases. An elegant model can be found by taking a Gaussian voltage pulse shape and a quadratic frequency dependent attenuation for elastic waves. With such a model it is not necessary to use Fourier transforms since an analytical time dependent solution exists. The voltage $V(t-\Delta t-z'/v_s)$ in Equation (4) has to be replaced by

$$\frac{V_m\,\sigma}{\sqrt{\sigma^2+4\alpha z'}}\,2^{-(t-\Delta t-z'/v_s)^2/(\sigma^2+4\alpha z')} \tag{11}$$

and $V^2(t-\Delta t-z'/v_s)$ by the square of this expression. The parameter V_m is the amplitude of the pulse voltage and 2σ is its width at amplitude $V_m/2$. The parameter α tunes how fast elastic waves attenuate. Various graphical representations of this function are shown in Figure 4. For causality, it is however necessary to take the origin of time not at the maximum of the pulse but at the beginning of the pulse. Since there is not a real beginning for a Gaussian pulse, one can take the time origin at $2^{-\beta^2}$ of the pulse amplitude. The lower the fraction, the lower the error. The voltage $V(t-\Delta t-z'/v_s)$ becomes

$$\frac{V_m\,\sigma}{\sqrt{\sigma^2+4\alpha z'}}\,2^{-(t-\Delta t-z'/v_s-\beta\sqrt{\sigma^2+4\alpha z'})^2/(\sigma^2+4\alpha z')} \tag{12}$$

It is fourthly necessary to discretize all continuous operators to calculate the signal.

Discretization begins by splitting the sample into `N` finite volume elements. In a one-dimensional model, the sample is then cut into `N` consecutive segments. Using MatLab [15] as the simulation software, the sample structure can then be described by a vertex point vector `z`, a center point vector `zc`, and an element dimension vector `dz`. Two consecutive components of vector `z` define respectively the beginning and the ending coordinates of an element of volume. Therefore vector `z` has `N+1` components. Each component of vectors `zc` or `dz` gives respectively the central coordinate and the dimension of an element of volume. Therefore vectors `zc` and `dz` have `N` components. The `N+1` components of vector `z` are initialized according to the sample structure and `z(N+1)-z(1)=`d. Vectors `zc` and `dz` are defined with vector `z` for instance as

```
zc = (z(1:N)+z(2:N+1))/2;
dz = diff(z);
```

Each volume element has its proper electrical parameters (ϵ and a) and conditions (ρ and π) which are assumed constant everywhere in the element. The permittivity `eps` (for ϵ), the electrostrictive coefficient `a` (for a), the charge density `rho` (for ρ), and the dipole density `p` (for π) are then vectors of `N` components. These vectors are initialized according to the electrical parameters and conditions of the sample.

From expressions (7), (10) and (9) and the applied voltage `Vapp` (for V_a), the electric field `E` (for E) can be calculated with

```
C0 = 1/sum(dz./eps);
C = C0*sum((cumtrapz(rho.*dz)-p).*dz./eps)+C0*Vapp;
E = (cumtrapz(rho.*dz)-p-C)./eps;
```

Discretization follows with time. Generally a constant time sampling period `dt` is used. Therefore the pulsed voltage `V` (for V) is a vector of `M` components, where `M*dt` is the measuring time window. In the expression (4) of the signal, the pulsed voltage appears with a constant delay Δt and a space dependent delay z'/v_s. In order to save memory space, it is possible to reduce the constant delay to zero ($\Delta t = 0$). Though this delay due to the elastic wave propagation through the waveguide is necessary in the real experiment, it is useless in the simulated experiment since electrical couplings and electromagnetic noises are not included in the simulation. As a consequence the `M` by `N` matrix representing the time-space dependences of V can be defined as

```
T = ones(N,1)*(0:M-1)*dt;
Z = zc'*ones(1,M);
Sigma = sqrt(sigma^2+4*alpha*Z);
V = Vm*sigma*2.^(-((T-Z/vs)./Sigma-beta).^2)./Sigma;
```

Notice that `Vm`, `sigma`, `alpha`, `beta` and `vs` stand respectively for V_m, σ, α, β and v_s which are used in expression (12).

The simulated signal `P` (for P) of Equation (4) can finally be calculated with

```
P = tau*C0/(2*vs*dt)*diff((((eps-a).*E+p)./eps.*dz)*V) ...
    -tau*C0^2/(4*vs*dt)*diff(((eps-a)./eps.^2.*dz)*(V.^2));
```

where the integration over the sample thickness of Equation (4) is made by a vector-matrix product.

2.4 Parameters of influence

The influence of the permittivity ϵ and the electrostrictive constant a can be evaluated by using a sample free of charge and of dipole, and submitted to an applied voltage V_a. In this case, the pressure at the transducer position is

$$P(t) = -\frac{\tau C_0^2}{4 v_s}\frac{\partial}{\partial t}\int_0^d \frac{\epsilon - a}{\epsilon^2} V(t-\Delta t - z'/v_s)\left[2V_a + V(t-\Delta t - z'/v_s)\right] \mathrm{d}z'. \tag{13}$$

Since the electrostrictive constant is of the order of $-\epsilon/2$ [16], the term $(\epsilon - a)/\epsilon^2$ presents discontinuities as many times as the permittivity presents discontinuities in the structure of the sample. Therefore, each discontinuity generates a signal. In a uniform sample **free of charge and dipole**, only the electrode interfaces present permittivity discontinuities so that the signal has only two peaks, one for the front electrode and the other for the back electrode. In the case of the sample structure of Figure 1, there are 6 discontinuities so that the signal presents 6 peaks, one for each interface. These peaks can thus be used as a source of information on the sample structure. **Knowing the thickness of each layer and the delay between each peak, it is possible to estimate the velocity of sound in each layer and thus the precise time-space correspondence. Conversely knowing the position in time of each peak, it is possible to precisely locate the layer in which an electrical phenomenon takes place that is exhibited at a given time in the signal.** Figure 5 shows a measured signal and the corresponding simulation. It can be noticed that, though the structure of Figure 1 is greatly simplified compared to the real sample structure and though elastic wave attenuation and dispersion have been simply modeled, simulated and measured signals are very similar.

For this simulation, each layer permittivity is a mixture of Epoxy resin and glass fibre permittivities, which are respectively to 25.5 pF/m and 59 pF/m. In this case the permittivity of layers 1 to 5 are respectively 30 pF/m, 50pF/m, 37pF/m, 50pF/m and 30pF/m, and the electrostrictive constant a is $-\epsilon/2$ in each layer. Concerning the other parameters, one has $V_a = +4000$ V, $V_m = +600$ V, $\sigma = 3.1$ ns, $\alpha = 3.4\,\sigma^2/d$, $\beta = 3$, $\tau = 0.14$ **mV/Pa when taking into account the transducer conversion coefficient and the 40 dB signal amplifier,** and $v_s = 3700$ m/s. Notice that the velocity of sound v_s used for the simulation depends on factors α and β which results in an overestimation of the real speed of sound. Since these latter parameters are associated with the properties and structure of the sample, and with the measurement setup, they will be used for all the simulations presented hereafter.

The influence of charge depends on where charges are trapped in the sample structure and thus on the buildup process. Studying all cases is of course out of the scope of this section. Instead we present in Figure 6 the influence of trapped charges at each interface which can be interpreted as injection, then migration, and finally trapping. The charge used for these simulations is $100\,\mu\mathrm{C/m^2}$ spread over 40 μm. In the case of injection of negative charges at the cathode (Figure 6a-left) the amplitude of the peak at the front electrode decreases and broadens whereas the others peaks in the signal are almost unchanged. Although less significantly visible, the same behavior can be observed in the case of injection of positive charges at the anode (Figure 6f-right). The peak at the back electrode indeed decreases and broadens and the other peaks remain almost unchanged. **When trapped at a distance smaller than the measurement spatial resolution from an interface between two layers**, negative charges (Figure 6b-left to e-left) shift down the corresponding peak but also decrease the amplitude of the peaks closer to the cathode and increase the peaks closer to the anode. Conversely positive charges (Figure 6b-right to e-right) shift up the peak where charges are trapped, increase the peaks closer to the cathode, and decrease the peaks closer to the anode.

The influence of the polarization of one layer in the sample structure is shown in Figure 7. The polarization used for these simulations is $-100\ \mu\text{C}/\text{m}^2$. It can be seen that the influence of polarization depends on the layer. Indeed in layers 1, 3 and 5 (Figure 7-left) where the permittivity is lower than the mean sample permittivity, **the peaks around the layer 1, 3 or 5 decrease** when the others increase, whereas in layers 2 and 4 (Figure 7-right) where the permittivity is larger than the mean sample permittivity, all peaks increase. Notice that a similar behavior can be obtained by combining positive and negative charges around one layer, that is to say the signals in Figure 6a-right to e-right with those in Figure 6b-left to f-left.

3 Measurements

3.1 Procedure

The sample described in section 2.1 has been stressed under 4 kV for one hour at room temperature. This voltage corresponds to a mean electric field of -10 kV/mm in the sample structure. Measurements with the PEA method have been carried out under stress and after stress in order to observe both buildup and decay of charges. **In order to increase the signal to noise ratio we averaged 1000 acquisitions by measurement.**

The signals presented in this paper were obtained with a sample without **bonded** electrodes. The aluminum waveguide and the carbon-loaded polymer electrode feeding the sample with the pulsed voltage act respectively as the front and the back electrodes. The acoustic couplings at both interfaces of the sample were obtained with silicone oil. It has been verified that the observed phenomena are not due to the absence of sample electrodes. In this study the absence of sample electrodes makes it possible to evaluate the influence on the position where measurements are carried out on the sample surface.

The contribution to the measured signal of the term in V^2 corresponding to the last integral of Equation (4) depends only on the sample structure and remains unaffected by the presence of charges or by the application of a voltage. This contribution can be determined by averaging two consecutive short-circuit measurements, the first being initiated by a positive pulsed voltage V and the second by a negative one. It can also be determined by the initial short-circuit measurement of the sample when it is free of charge and dipole. For sake of simplicity in the signal analysis, the contribution of the term in V^2 has been removed in all the signals shown hereafter.

3.2 Results and descriptions

For sake of clarity in the descriptions, we refer hereafter to peak 1, 2, 3, 4, 5 or 6 as the peak in the signal generated at the front electrode, at the interfaces between layers 1 and 2, layers 2 and 3, layers 3 and 4, layers 4 and 5, and at the back electrode respectively.

The signals obtained under voltage are presented in Figure 8. The signal evolves everywhere in the structure but with different rates. The evolution is indeed rapid and then stopped for peaks 3 and 4, whereas it is gradual over the hour of stress for peaks 1, 2, 5 and 6. At the same time the rapid evolution is associated with an increase of the peak amplitudes whereas the gradual evolution is associated with a decrease of the peak amplitudes.

The decay after the voltage stress is shown in Figure 9. As for the buildup, two different evolutions can be observed. The first evolution is rapid and concerns peaks 3 and 4, and the second evolution is gradual and concerns peaks 1, 2, 5 and 6. In addition the peaks varying rapidly in amplitudes first invert and then decay slowly approximatively at the same rate as that of the gradual evolution.

Since different buildup processes seem to happen, other measurements under 4 kV were carried out at a different position on the sample surface in order to evaluate if variations in the fibre distribution is of influence. Prior to this measurement the sample was unloaded from and reloaded into the sample holder, and short-circuited a sufficient period of time to remove all the remaining charges. The first signals obtained under voltage are presented in Figure 10. The behavior has changed with the measurement position since all peaks increase, with a larger increase for the inner peaks (2, 3, 4 and 5) than for the interfacial peaks (1 and 6).

4 Analysis and discussion

Figures 8 and 9 show clearly two processes, one rapid and the other gradual. **It has been shown [17] that conduction in or on silica fibres is larger than in Epoxy resin. That difference in conduction can be at the origin of the observed difference in the dynamics of these two processes. In the following the rapid and the slow processes are treated independently**.

The rapid increase of peaks 3 and 4 under voltage can be simulated by adding negative charges at interface 3 (see Figure 6c-left) and positive charges at interface 4 (see Figure 6d-right). Since the other peaks increase with only these charges whereas in the measurement (see Figure 8) they remain unchanged except for the interfacial peaks which slightly decrease, a small amount of positive and negative charges have to be placed in layers 1 and 5 respectively. The signal at 10 minutes shown in Figure 11 has been simulated with $-85\,\mu\text{C/m}^2$ at the cathode (interface 1) $+39\,\mu\text{C/m}^2$ at interface 2, $-124\,\mu\text{C/m}^2$ at interface 3, $+57\mu\text{C/m}^2$ at interface 4, $0\,\mu\text{C/m}^2$ at interface 5 and $+57\,\mu\text{C/m}^2$ at the anode (interface 6). Insofar as there is no chance for these charges to buildup directly at these interfaces, they should have migrated or been injected. We propose that fibre layers polarize or dissociate charges rapidly owing to their relatively large conductivity **(Figure 13a)**. Then positive charges at interface 2 are almost neutralized by fast injection and migration from the cathode, and negative charges at interface 5 are neutralized by fast injection (extraction) and migration from the anode **(Figure 13b). This would be responsible for the rapid change in the signal.**

Once the rapid process has stabilized, a slower process becomes dominant. The decrease of the interfacial peaks and of peak 2 can be simulated by adding negative charges at interface 2 and positive charge at interface 5 (see Figure 6b-left and e-right). The signal at 60 minutes shown Figure 11 has been simulated by adding to the previous charges $-106\,\mu\text{C/m}^2$ at interface 2 and $+106\,\mu\text{C/m}^2$ at interface 5. We suggest that injection continues and that charges migrate **and** then are trapped at interface 1 for injection from the cathode, and at interface 5 for injection from the anode **(Figure 13c). This would be responsible for the gradual change in the signal.**

Under short-circuit, rapid and gradual processes are visible at the same interfaces as under voltage. The rapid process can be simulated by changing the polarity of the charges at interface 3 and 4 since the corresponding peaks invert in the signal (see Figure 9). At the same time positive charges at interface 2 and 5 have to be removed to take into account the evolution of the corresponding peaks. The signal after 10 minutes of Figure 12 has been simulated with $+35\,\mu\mathrm{C/m}^2$ at interface 3, and $-18\,\mu\mathrm{C/m}^2$ at interface 4 and by removing $+35\,\mu\mathrm{C/m}^2$ at interfaces 2 and 5. We conclude that charges have continued to migrate in the structure from the cathode and from the anode under voltage and that once the applied voltage was removed the polarization or the charge dissociation in the fibre mat diminishes and gives place to the migrated charges **(Figure 13d)**. Then charges remaining in the structure recombine slowly **(Figure 13e)**. The signal at 60 minutes has been simulated by dividing all charges by a factor 2. **As under voltage, silica fibres would be at the origin of the rapid process whereas Epoxy resin at the origin of the gradual process.**

The measurements at another position on the sample surface presented in Figure 10 show a different behavior for the rapid evolution of the peaks. Indeed they all increase with a larger increase for peaks 2, 3, 4 and 5. This rapid process can be simulated with just a polarization or a dissociation of charge in the fibres as shown in Figure 14. We suggest that the injection of charges has not occurred in this experiment due to the slight modification in position, and thus in the fibre distribution, compared to the previous experiment. The difference in behavior can be attributed for instance to fibres that approach more or less the electrodes **as illustrated in Figure 15**. When fibres are close to an electrode, charges can inject or extract easily**, move along fibres easily,** and then compensate or recombine with the dissociated charges in the fibres. The divergent electric field fibres produce in their vicinity can promote such a behavior. When fibres are not close to an electrode, the exchange with the interface is less easy and only the dissociated charges in the fibres are visible. **As a consequence we propose that the fast injections assumed to explain one part of the rapid process in Figure 8 would have been made easier by the presence of fibres close to the interfaces during the measurement. In Figure 10 the absence of fibres close to an interface would have restrained the injection so that second peak increases instead of decreasing.**

5 Conclusions

In this paper we have shown how space charge dynamics in complex laminates may be simulated and also that, even if the simulated signals do not match the measured ones perfectly, a clear idea of the charge processes occurring can be **deduced**. The slight discrepancy between measured and simulated signals is due to the simplifications made to model the sample structure and the wave propagation.

We have studied an Epoxy resin board including a fibre mat and have shown that under voltage two processes with different dynamics are visible. **We propose that the rapid process is** attributed to charge dissociations in the fibres and the slow process to charge **migrations** in the Epoxy layers close to the electrodes. In addition we **suggest** that when fibres are close to an electrode, charge injection or extraction is highly facilitated.

In such laminate samples, the signal is very complex to analyze due to the response induced by the spatial variations of the sample properties, at least permittivity. The simulation proposed in this paper brings a great help to understand where charges are in the sample structure.

References

[1] L.A. Dissado, G. Mazzanti, and G.C. Montanari. The role of trapped space charges in the electrical aging of insulating materials. *IEEE Trans. Dielectr. EI*, 4:496–506, 1997.

[2] G. Keiser. *Optical Fibre Communications.* McGraw-Hill, USA, 2000.

[3] T. Mizutani. Space charge techniques and space charge in polyethylene. *IEEE Trans. Dielectr. EI.*, 1:923–933, 1994.

[4] T. Maeno, H. Kushiba, T. Takada, and C. M. Cooke. Pulsed electro-acoustic method for the measurement of volume charge in e-beam irradiated PMMA. In *Conference on Electrical Insulation and Dielectric Phenomena*, pages 389–397, Amherst NY, USA, 1985. IEEE.

[5] J. B. Bernstein. Analysis of the electrically stimulated acoustic-wave method for observing space charge in semi-insulating films. *Phys. Rev. B*, 44:804–814, 1991.

[6] P. Laurenceau, G. Dreyfus, and J. Lewiner. New principle for the determination of potential distributions in dielectrics. *Phys. Rev. Lett.*, 38:46–49, 1977.

[7] C. Alquié, G. Dreyfus, and J. Lewiner. Stress wave probing of electric field distributions in dielectrics. *Phys. Rev. Lett.*, 47:1483–1487, 1981.

[8] G. M. Sessler, J. E. West, and R. Gerhard-Multhaupt. Measurement of charge distribution in polymer electrets by a new pressure-pulse method. *Polym. Bull.*, 6:109–111, 1981.

[9] S. Holé, T. Ditchi, and J. Lewiner. Non-destructive methods for space charge distribution measurements: what are the differences? *IEEE Trans. Dielectr. EI.*, 10:670–677, 2003.

[10] S. Holé, T. Ditchi, and J. Lewiner. Influence of divergent fields on space charge distribution measurements using elastic methods. *Phys. Rev. B*, 61:13528–13539, 2000. In Eq. (21) B_k should be E_k and in Eq. (47) ϵ_j should be ξ_j.

[11] S. Holé, A. Sylvestre, C. Guillermin, P. Rain, and S. Rowe. Space charge measurement on filled epoxy. In *8th International Conference on Solid Dielectrics*, pages 154–157, Toulouse, France, 2004. IEEE Pub. CH37539.

[12] S. Holé, V. Griseri, L.A. Dissado, and J.C. Fothergill. Improvement of PEA signal analysis using simulations for complex geometry samples. *J. Phys. D:Appl. Phys.*, 35:19–24, 2002.

[13] P.A. Lynn and W. Fuerst. *Introductory digital signal processing with computer applications (2nd rev. ed.).* John Wiley, UK, 1998. ISBN: 0471976318.

[14] T. Ditchi, C. Alquié, and J. Lewiner. Broadband determination of ultrasonic attenuation and phase velocity in insulating materials. *J. Acoust. Soc. Am.*, 94:3061–3066, 1993.

[15] Amos Gilat. *Matlab: An Introduction With Applications.* John Wiley & Sons, Indianapolis, IN, USA, 2004.

[16] K. Nakamura and Y. Wada. Piezoelectricity, pyroelectricity and electrostriction constant in PVF. *J. Polym. Sci.*, 9:161–173, 1971.

[17] M.N. Ajour, L.A. Dissado, J.C. Fothergill, and P.N. Norman. Dielectric spectroscopy of epoxy/glass composite materials. In *Conference on Electrical Insulation and Dielectric Phenomena*, pages 438–441. IEEE Annual report, 2002.

Figure 1: Cut-section of the **laminate sample. Left: micro-photograph with silica fibres appearing in white and Epoxy resin in grey. Right: simplified model of the sample structure**.

Figure 2: **PEA Setup. A pulsed voltage V causes the charges in the sample to generate elastic waves which are measured by an adjacent transducer. The signal produced by the transducer is the image of the charge in the sample.**

Figure 3: Signal under 4-kV applied voltage with a 1-mm-thick semi-conductive electrode at the back of the sample. Notice that the short-circuit measurement has been removed in the signal presented.

Figure 4: Model for a Green's function including an attenuation parameter.

Figure 5: Comparison between measured and simulated signals for a laminate.

Figure 6: Effect of negative (left) and positive (right) charges. (a) charges at the cathode, (b) charges at interface 2, (c) charges at interface 3, (d) charges at interface 4, (e) charges at interface 5, and (f) charges at the anode.

Figure 7: Effect of one layer polarization. (a) polarization of layer 1, (b) polarization of layer 2, (c) polarization of layer 3, (d) polarization of layer 4, and (e) polarization of layer 5.

Figure 8: Signal evolution during the 4-kV stress.

Figure 9: Signal evolution during the decay after a one hour 4-kV stress.

Figure 10: Signal evolution during the 4-kV stress at a different position in the sample.

Figure 11: Simulated signal buildup. **Inset: space charge distributions used for the simulation.**

Figure 12: Simulated signal decay. **Inset: space charge distributions used for the simulation.**

Figure 13: **Assumed charge behavior under voltage and short circuit. (a) dissociation in fibres, (b) fast injection and migration, (c) slow migration, (d) recombination of charges in fibres, and (e) decay of charges in Epoxy resin.**

Figure 14: Simulated signal buildup at a different position in the sample. **Inset: space charge distributions used for the simulation.**

Figure 15: **Assumed charge behaviour at different locations. (a) injection and migration facilitated by the presence fibres close to the interface, (b) difficult migration through a thick layer of Epoxy resin.**

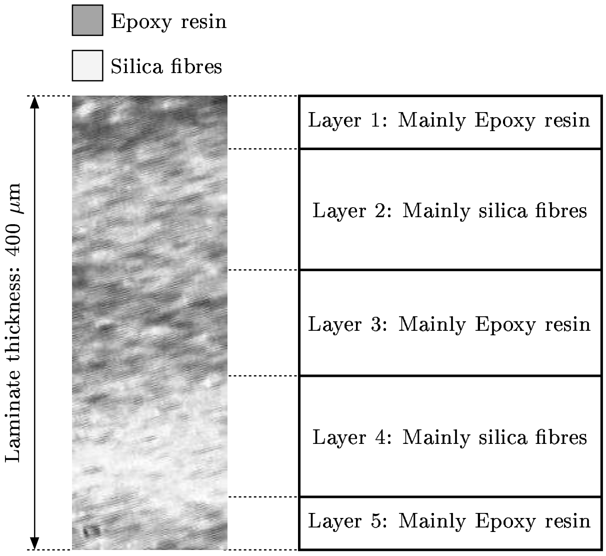
Epoxy resin
Silica fibres
Laminate thickness: 400 μm
Layer 1: Mainly Epoxy resin
Layer 2: Mainly silica fibres
Layer 3: Mainly Epoxy resin
Layer 4: Mainly silica fibres
Layer 5: Mainly Epoxy resin

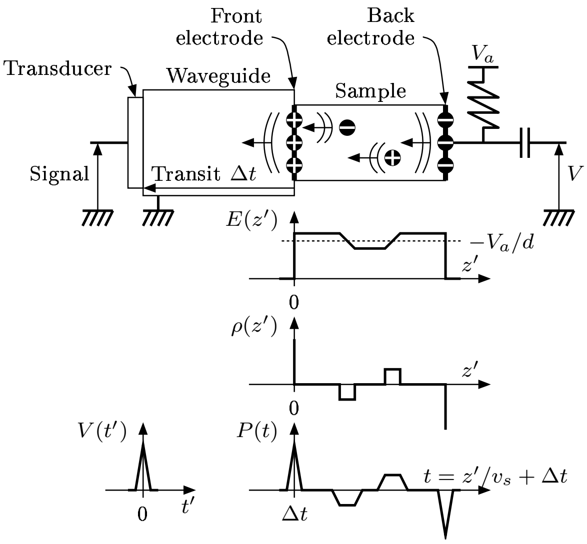
Front electrode
Back electrode
Transducer
Waveguide
Sample
V_a
Signal
Transit Δt
V
$E(z')$
$-V_a/d$
z'
0
$\rho(z')$
z'
0
$V(t')$
0
t'
$P(t)$
$t = z'/v_s + \Delta t$
Δt

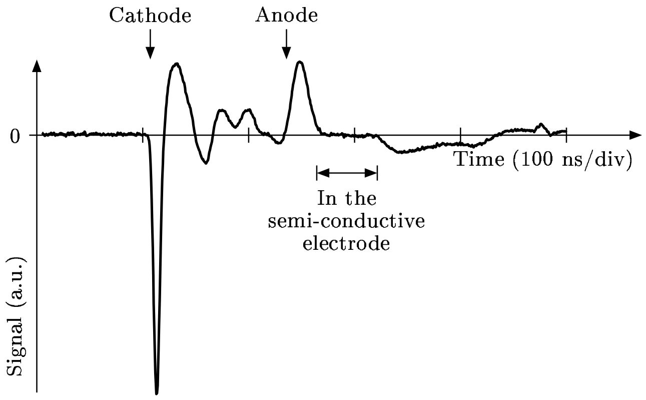
Cathode
Anode
0
Time (100 ns/div)
In the
semi-conductive
electrode
Signal (a.u.)

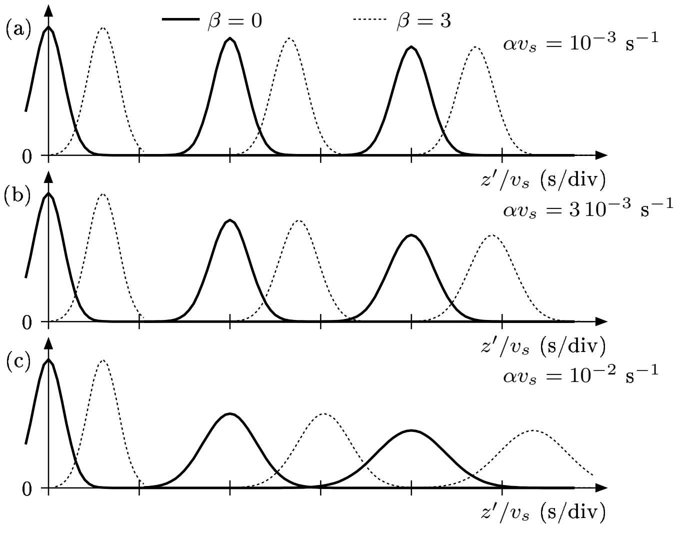
(a)
$\beta = 0$
$\beta = 3$
$\alpha v_s = 10^{-3}\ \mathrm{s}^{-1}$
0
z'/v_s (s/div)
(b)
$\alpha v_s = 3\,10^{-3}\ \mathrm{s}^{-1}$
0
z'/v_s (s/div)
(c)
$\alpha v_s = 10^{-2}\ \mathrm{s}^{-1}$
0
z'/v_s (s/div)

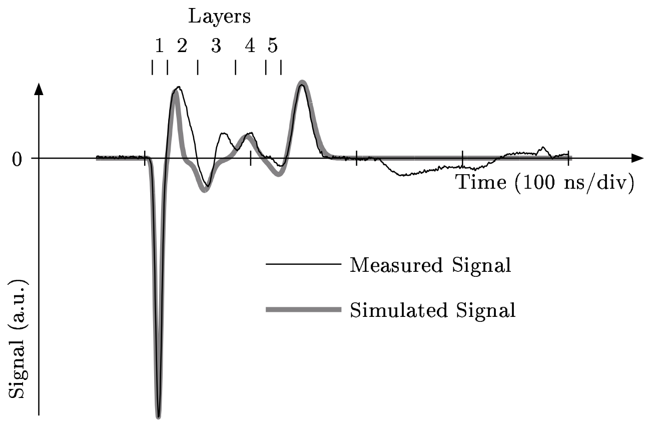
Layers
1
2
3
4
5
0
Time (100 ns/div)
Signal (a.u.)
Measured Signal
Simulated Signal

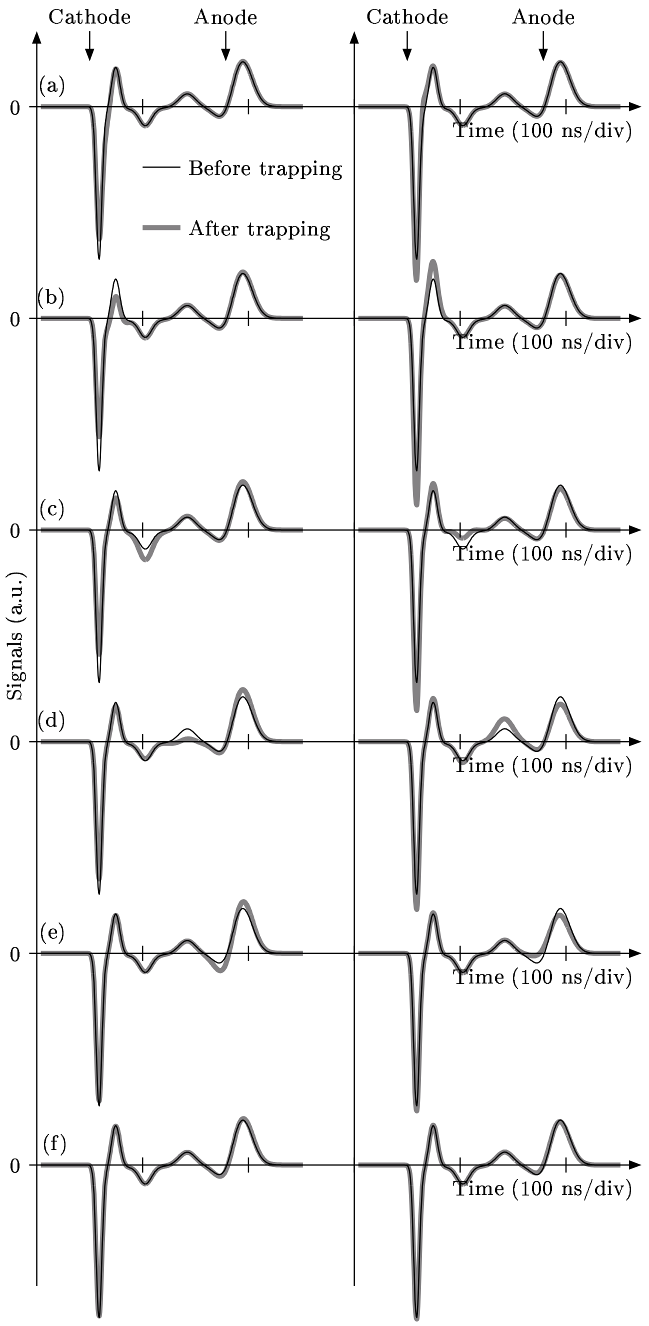
Cathode
Anode
Cathode
Anode
(a)
0
Time (100 ns/div)
Before trapping
After trapping
(b)
0
Time (100 ns/div)
(c)
0
Time (100 ns/div)
Signals (a.u.)
(d)
0
Time (100 ns/div)
(e)
0
Time (100 ns/div)
(f)
0
Time (100 ns/div)

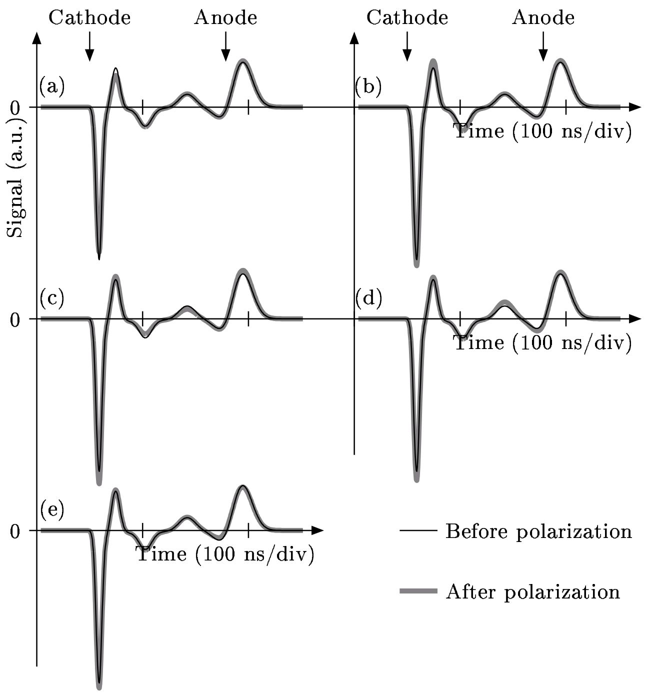
Cathode
Anode
Cathode
Anode
(a)
(b)
0
Signal (a.u.)
Time (100 ns/div)
(c)
(d)
0
Time (100 ns/div)
(e)
0
Time (100 ns/div)
Before polarization
After polarization

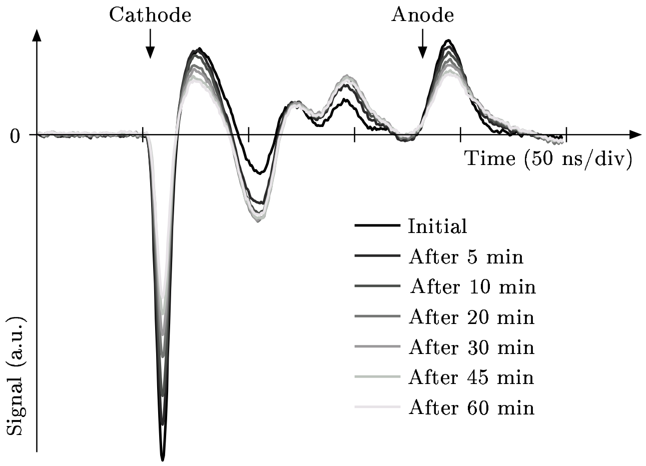
Cathode
Anode
0
Time (50 ns/div)
Signal (a.u.)
Initial
After 5 min
After 10 min
After 20 min
After 30 min
After 45 min
After 60 min

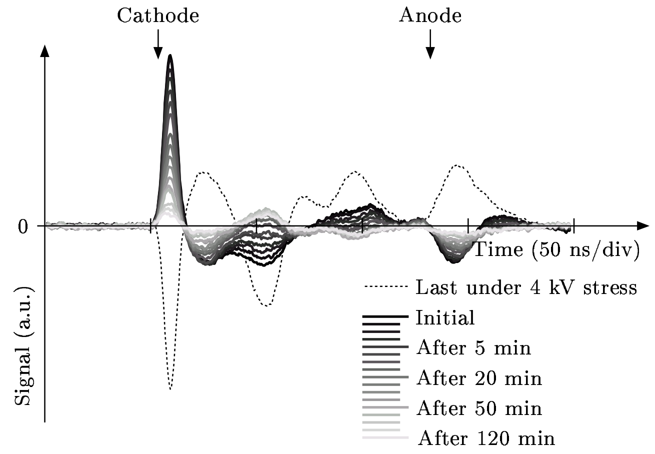
Cathode
Anode
0
Signal (a.u.)
Time (50 ns/div)
Last under 4 kV stress
Initial
After 5 min
After 20 min
After 50 min
After 120 min

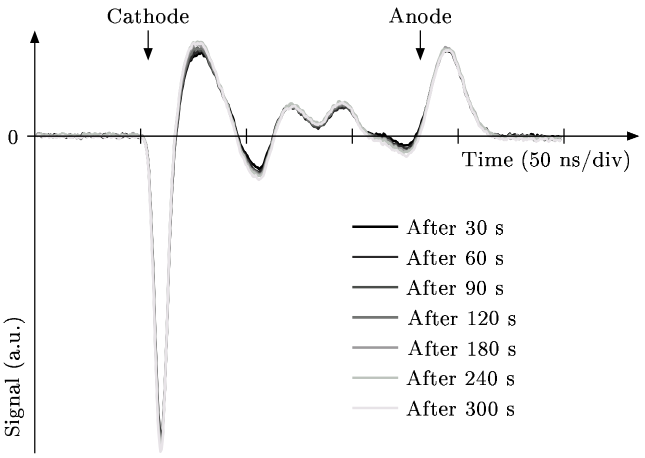
Cathode
Anode
0
Time (50 ns/div)
Signal (a.u.)
After 30 s
After 60 s
After 90 s
After 120 s
After 180 s
After 240 s
After 300 s

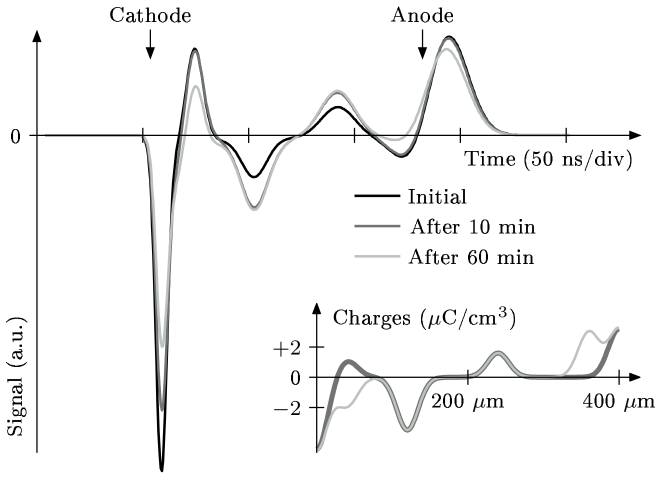
Cathode
Anode
0
Time (50 ns/div)
Signal (a.u.)
Initial
After 10 min
After 60 min
Charges (μC/cm³)
+2
0
−2
200 μm
400 μm

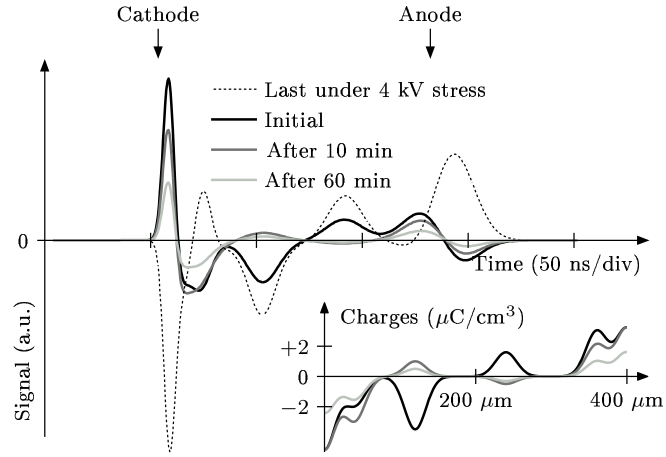
Cathode
Anode
Last under 4 kV stress
Initial
After 10 min
After 60 min
0
Time (50 ns/div)
Signal (a.u.)
Charges (μC/cm^3)
+2
0
−2
200 μm
400 μm

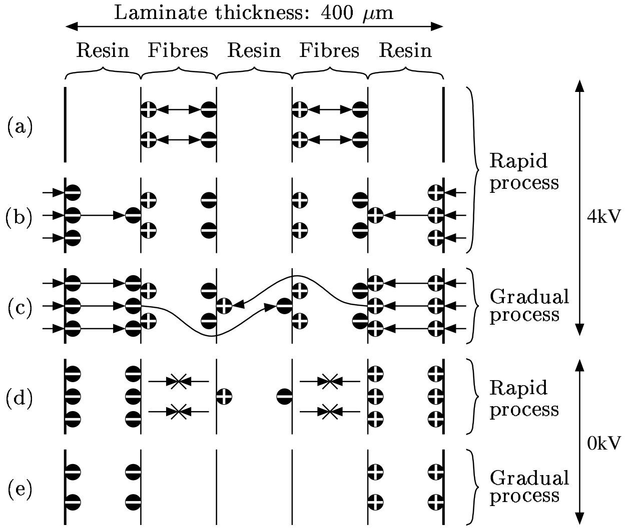
Laminate thickness: 400 μm
Resin
Fibres
Resin
Fibres
Resin
(a)
(b)
(c)
(d)
(e)
Rapid process
Gradual process
Rapid process
Gradual process
4kV
0kV

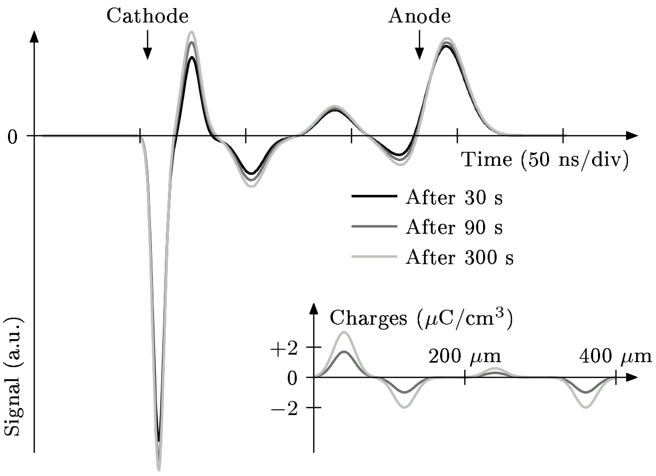
Cathode
Anode
0
Time (50 ns/div)
Signal (a.u.)
After 30 s
After 90 s
After 300 s
Charges (μC/cm^3)
+2
0
−2
200 μm
400 μm

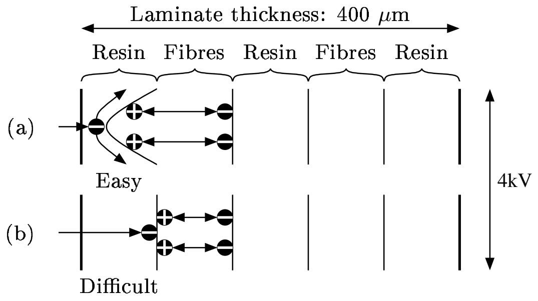
Laminate thickness: 400 μm
Resin
Fibres
Resin
Fibres
Resin
(a)
Easy
(b)
Difficult
4kV